Biomechan Model Mechanobiol (2006) 5: 180–191
DOI 10.1007/s10237-006-0020-7

ORIGINAL PAPER

M.M. Knight · Z. Bomzon · E. Kimmel · A.M. Sharma
D.A. Lee · D.L. Bader

Chondrocyte deformation induces mitochondrial distortion and heterogeneous intracellular strain fields

Received: 21 March 2005 / Accepted: 3 August 2005 / Published online: 7 March 2006

Abstract Chondrocyte mechanotransduction is poorly understood but may involve cell deformation and associated distortion of intracellular structures and organelles. This study quantifies the intracellular displacement and strain fields associated with chondrocyte deformation and in particular the distortion of the mitochondria network, which may have a role in mechanotransduction. Isolated articular chondrocytes were compressed in agarose constructs and simultaneously visualised using confocal microscopy. An optimised digital image correlation technique was developed to calculate the local intracellular displacement and strain fields using confocal images of fluorescently labelled mitochondria. The mitochondria formed a dynamic fibrous network or reticulum, which co-localised with microtubules and vimentin intermediate filaments. Cell deformation induced distortion of the mitochondria, which collapsed in the axis of compression with a resulting loss of volume. Compression generated heterogeneous intracellular strain fields indicating mechanical heterogeneity within the cytoplasm. The study provides evidence supporting the potential involvement of mitochondrial deformation in chondrocyte mechanotransduction, possibly involving strain-mediated release of reactive oxygen species. Furthermore the heterogeneous strain fields, which appear to be influenced by intracellular structure and organisation, may generate significant heterogeneity in mechanotransduction behaviour for cells subjected to identical levels of deformation.

M.M. Knight (✉) · A.M. Sharma · D.A. Lee · D.L. Bader
Medical Engineering Division,
Dept. of Engineering and IRC in Biomedical Materials,
Queen Mary University of London,
London, UK
E-mail: m.m.knight@qmul.ac.uk
Tel: 44-20-7882-5512
Fax: 44-20-8983-1799

Z. Bomzon · E. Kimmel
Faculty of Civil & Environmental Engineering,
Technion Israel Institute of Technology,
Haifa, Israel

E. Kimmel
Department of Biomedical Engineering,
Technion Israel Institute of Technology,
Haifa, Israel

1 Introduction

Articular chondrocytes are highly specialised cells that are able to detect changes in their mechanical environment and respond by altering the synthesis and catabolism of the extracellular matrix in order to maintain functional articular cartilage. Numerous previous studies, both in vivo and in vitro, have demonstrated that static compression down regulates chondrocyte matrix production, while some modes of cyclic compression can produce an up regulation of matrix production. However, the precise intracellular signalling pathways associated with mechanotransduction are as yet unclear. Physiological loading of cartilage produces cell deformation, increased hydrostatic pressure, fluid shear, electrical streaming potentials and changes in pH and osmotic pressure (see Urban 1994 for review). Cell deformation per se may trigger distortion of cellular structures such as the nucleus (Guilak 1995), endoplasmic reticulum (Szafranski et al. 2004), cytoskeleton and integrins (Mobasheri et al. 2002; Millward-Sadler and Salter 2004). Such events may then produce either direct changes in gene expression or protein synthesis or may activate signalling cascades such as those involving intracellular calcium (Guilak et al. 2000; D'Andrea et al. 2000; Roberts et al. 2001). Recently it has been suggested that distortion of the mitochondria may be involved in mechanotransduction, possibly through the strain-activated release of reactive oxygen species (Ali et al. 2004; Szafranski et al. 2004). However, little is known of how the mitochondria respond to compression in living cells. This aim of this study is therefore to test the hypothesis that chondrocyte deformation induces heterogeneous intracellular strains and associated distortion of the mitochondrial network.

The study uses a well-characterised in vitro model system consisting of isolated chondrocytes cultured within agarose gel (Lee et al. 2000). Using this model system, it has been

shown that gross compression generates uniform homogeneous cell deformation, a necessary prerequisite for examining issues of intracellular heterogeneity. An optimised digital image correlation (DIC) technique has been developed to quantify the movement and distortion of the mitochondrial network using live cell confocal microscopy. This computational approach is similar to that adopted in previous studies which have examined the influence of mechanical stimuli on endothelial cells (Helmke et al. 2000, 2001, 2003), smooth muscle cells (Hu et al. 2003) and fibroblasts (Delhaas et al. 2002). However, the present study is the first to quantify the intracellular mechanical environment within viable articular chondrocytes subjected to physiological compression and in so doing investigate mitochondria deformation which may be involved in cartilage mechanotransduction.

2 Method

2.1 Preparation of chondrocyte-agarose constructs

Isolated bovine articular chondrocytes were embedded within a 3D agarose gel as previously detailed (Lee et al. 2000; Lee and Bader 1997). To review briefly, articular chondrocytes were isolated from the metacarpal–phalangeal joint of adult steers aged between 18 and 30 months, using a well established sequential enzyme digestion protocol with pronase and collagenase (Lee and Bader 1997). The isolated chondrocytes were seeded at 10×10^6 cells/ml in 3% agarose gel (Sigma, Poole, UK) and gelled for 20 min at 4°C between porous glass endplates in specially designed moulds. This created identical rectangular cell-agarose constructs, $5\times5\times5\,mm^3$, with porous glass endplates $5\times5\times4\,mm^3$, attached to each end, as previous described (Sawae et al. 2004). The cell-agarose constructs were cultured overnight at 37°C and 5% CO_2 in sterile Dulbecco's modified Eagles medium plus 20% foetal calf serum supplemented with 2 mM l-glutamine, 20 mM HEPES, 50 μg/ml penicillin, 50 μg/ml streptomycin and 150 μg l-ascorbic acid (DMEM+20%FCS, all from Sigma).

2.2 Mitochondria-cytoskeletal co-localisation

At day 1 of culture, cell-agarose constructs were cut transversely into 1 mm thick slices using a scalpel and incubated for 3 h at 37°C in a 200 nM solution of Mitotracker Red, CMXRos (Molecular Probes) in DMEM+20%FCS. The resulting specimens were fixed in 4% paraformaldehyde at 37°C for 15 min and washed in phosphate buffered saline (PBS, Sigma). Specimens were then incubated at 4°C for 5 min in permeablising buffer consisting of 10.3 g sucrose, 0.292 g sodium chloride, 0.006 g magnesium chloride, 0.476 g HEPES and 0.5 ml Triton X dissolved in 100 ml distilled water (Idowu et al. 2000; Lee et al. 2000). Specimens were then washed for 5 min in PBS + 1% bovine serum albumin (BSA, Sigma). Separate specimens were used for co-localisation of mitochondria with each of the three cytoskeletal networks. F-Actin present within actin microfilaments was directly labelled by incubating in 2 μM of FITC conjugated Phalloidin (Molecular Probes) in PBS + 1% BSA. Indirect immunofluorescence was used to label vimentin intermediate filaments and microtubules using monoclonal primary antibodies, anti-vimentin (clone V9, Sigma) and anti-β tubulin (clone TUB2-1, Sigma), respectively, as described previously (Idowu et al. 2000; Lee et al. 2000). Confocal z-series of dual labelled cells were recorded with a x60/0.95 NA oil immersion objective lens.

2.3 Visualisation of mitochondrial deformation

At day 1 of culture, cell-agarose constructs were incubated in Mitotracker Red, CMXRos (200 nM, 1 h, 37°C, Molecular Probes) in DMEM+20%FCS. Constructs were washed briefly in DMEM+20%FCS and mounted in a computer controlled compression rig, similar to that previously described (Roberts et al. 2001). The porous glass endplates at each end of the cell-agarose construct were gripped by two platens and the construct immersed in bicarbonate-free DMEM+20%FCS (Sigma), maintained at 37°C. The compression rig was placed on the stage of an inverted microscope (TE-Eclipse, Nikon, Kingston-upon-Thames, UK) associated with a confocal system (UltraView, Perkin Elmer, Cambridge, UK). Confocal imaging of fluorescently labelled mitochondria in individual cells was performed using a x60/0.95 NA oil immersion objective lens, yielding a pixel size of $0.13\times0.13\,\mu m$. Confocal images bisecting the centre of an individual cell in the unstrained state were recorded every 2 min along with corresponding brightfield images. A set of five image pairs were recorded over an 8 min period showing the cell in the uncompressed state. The cell-agarose construct was then subjected to increments of gross compressive strain applied every 2 min, while continuously tracking an individual cell. Further confocal and brightfield image pairs of the same cell were recorded at 3, 5, 10, and 15% gross strain, in a protocol shown schematically in Fig. 1. The procedure was repeated for a total of 10 cells, each time using a separate cell-agarose

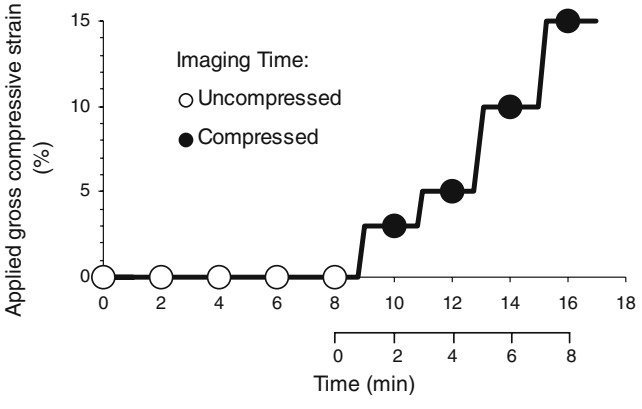

Fig. 1 Schematic diagram showing the protocol employed for imaging cells in uncompressed and compressed agarose constructs

construct. In all cases, cells were selected in the central region of the construct, approximately 20–50 μm from the surface closest to the coverslip. In this region, gross compression generates uniform local strain fields approximately equal to the applied strain (Knight et al. 1998). Furthermore, optical quality is optimised by minimising the distance between the cell and the objective lens. Within this region, individual cells were selected for maximum brightness, clarity and density of mitochondrial features within the confocal section bisecting the centre of the cell.

In a separate experiment, time-lapse confocal imaging was used to visualise the dynamics of mitochondria in chondrocytes maintained in either an uncompressed or a compressed state for a 10-min period. Confocal images of individual cells were recorded every 10 s following the onset of a 15% gross compressive strain. Control cells were visualised in an identical manner in separate uncompressed constructs. The movement and reorganisation of mitochondrial features was quantified using digital image correlation to compare images obtained at the start and end of the 10 min period.

2.4 Quantification of intracellular displacement and strain fields using Digital Image Correlation

The intracellular displacements and strains were calculated based on the movement and distortion of the mitochondria, which was analysed using an optimised DIC technique similar to that recently described (Wang and Cuitino 2002). Confocal images were saved in TIF format and exported into MatLab 6.5® software. For each image, a Sobel edge detection filter was applied and regions of interest (ROIs) with a size of 17×17 pixels were created, centred around 500 randomly selected pixels on the detected edges. DIC calculates the transformation, T, which converts a reference image $F(X)$ to a deformed image $G(x)$, with X and x denoting coordinates in the reference and deformed configurations, respectively. The transformation was calculated in each ROI using a Newton–Raphson optimization algorithm (Wang and Cuitino 2002) in order to minimise the difference between $F(T(X))$ and $G(x)$, as defined in Eq. (1);

$$\chi^2 = \frac{\sum\sum |F(T(X)) - G(x)|^2}{\sqrt{\sum\sum F(TX)^2 \sum\sum G(x)^2}}. \quad (1)$$

The summation is performed over all pixels in the ROI, and T is assumed to have the form,

$$\begin{pmatrix} x \\ y \end{pmatrix} = T(X,Y) = \mathbf{F}(\mathbf{X} - \mathbf{X}_c) + \mathbf{u}_c = \mathbf{F}\begin{bmatrix} X - X_c \\ Y - Y_c \end{bmatrix} + \begin{bmatrix} u_{xc}, \\ u_{yc} \end{bmatrix}, \quad (2)$$

where X_c indicates the centre of the ROI, u the displacement of X_c, and $\mathbf{F}$ may be defined as follows:

$$\mathbf{F} = \begin{bmatrix} \frac{\partial x}{\partial X} & \frac{\partial x}{\partial Y} \\ \frac{\partial y}{\partial X} & \frac{\partial y}{\partial Y} \end{bmatrix}. \quad (3)$$

The DIC technique was performed on pairs of images made at 2 min intervals in both the uncompressed state and at incremental levels of compression. The accumulative deformation from the initial, uncompressed state was calculated by summing the resulting displacements. This incremental approach ensured that the relative difference between a pair of images was sufficiently small to maintain the accuracy and convergence of the DIC algorithm. For ROIs in which the DIC algorithm did not converge, the data was discarded. DIC was also performed on confocal images made at the start and end of the 10 min period at either 0 or 15% gross compressive strain.

The partial derivatives obtained with DIC (Eq. 3) represent the average strain values for each ROI. The derivatives obtained with DIC strongly depend on local intensity variations. Consequently, it was more accurate to calculate intracellular strains directly from the displacements. This was achieved by fitting a thin-plate smooth spline to the displacement data using the Matlab spline toolbox. This involved employing Delaunay triangulation to draw the smallest possible set of triangles to connect the centres of all ROIs. The displacements of the vertices of these triangles defined a set of three linear equations for each triangle. These equations were solved to yield the components of the Strain tensors parallel and perpendicular to the axis of compression within the respective triangle.

A visual representation of the magnitudes of displacements within the cells was obtained by interpolating the values of displacements throughout the cell, and creating a psuedocolour map. Dark blue indicated no displacements, whereas red indicated a larger magnitude of displacement. Pseudocolour maps were also created to depict local strains throughout the cell, such that red indicates a positive strain or expansion and blue indicates a negative strain or compression. Areas in which no discernable mitochondrial features were present were left black. This was achieved by first thresholding the original image to highlight the mitochondrial features. All pixels at a distance of greater than five pixels from these features were left black in the psedocolour maps.

3 Results

3.1 Mitochondrial organisation and cytoskeletal co-localisation

Confocal imaging and fluorescent labelling with Mitotracker revealed that mitochondria formed a fibrous network or reticulum in isolated chondrocytes cultured in agarose constructs (Fig. 2). This reticulum structure was particularly evident when visualised in a 3D reconstruction of confocal z series (Fig. 2m). The organisation of the mitochondrial network varied considerably throughout the cytoplasm and also from cell to cell. However, the mitochondria generally appeared more densely organised in the perinuclear region. Dual confocal imaging of cells indicated partial co-localisation between the

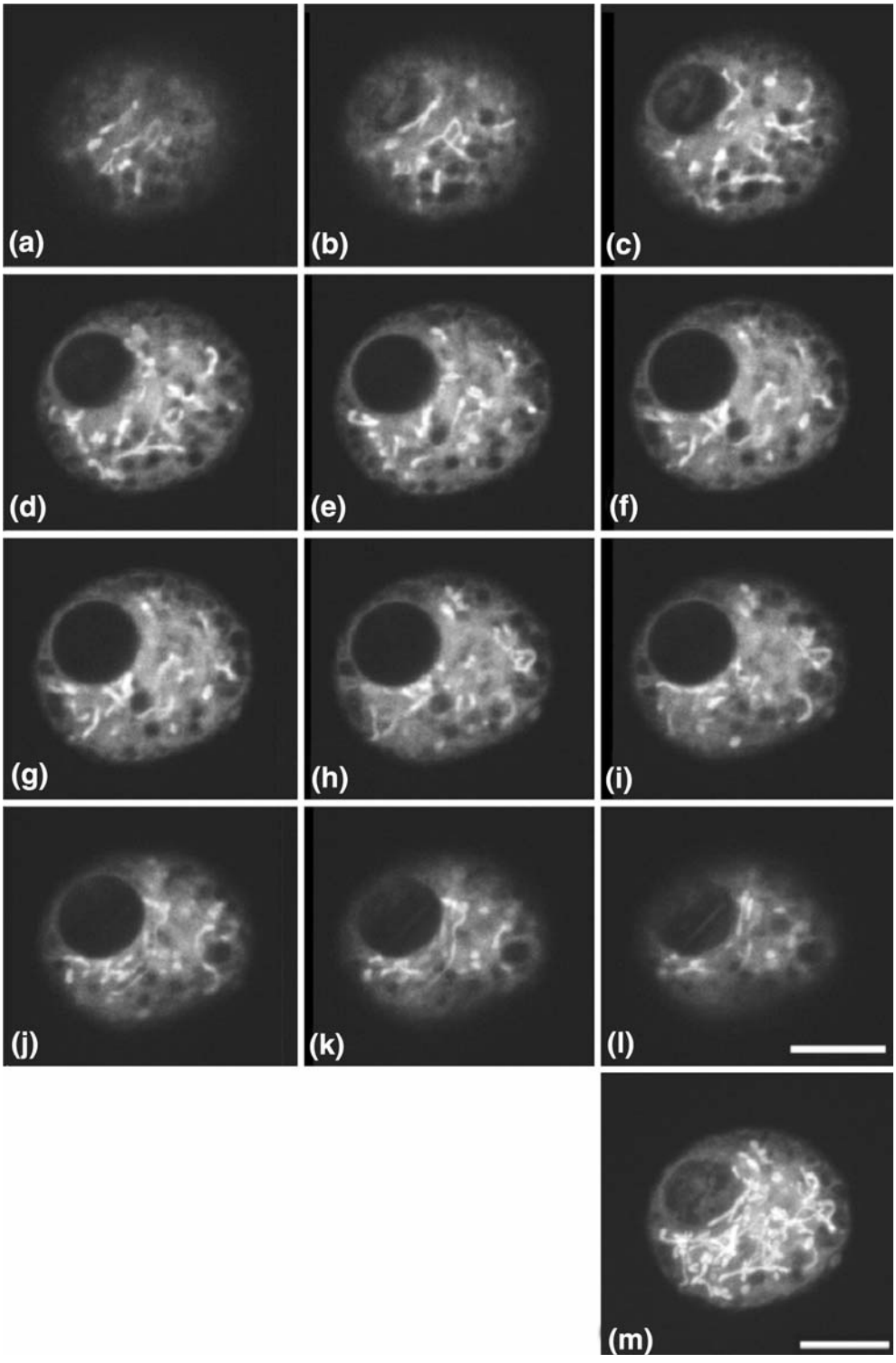

Fig. 2 Organisation of the mitochondria within an isolated chondrocyte in an uncompressed agarose constructs. Confocal *z*-series throughout the thickness of the cell (**a**–**l**) and 3D reconstruction image (**m**). *Scale bar* represents 5 μm

mitochondria and both the microtubules and the vimentin intermediate filaments (Fig. 3). However, there was no evidence of co-localisation between the mitochondria and actin microfilaments.

3.2 Mitochondrial deformation and intracellular mechanics

Isolated chondrocytes cultured for 24 h in uncompressed agarose constructs exhibited a spherical morphology with no dis-

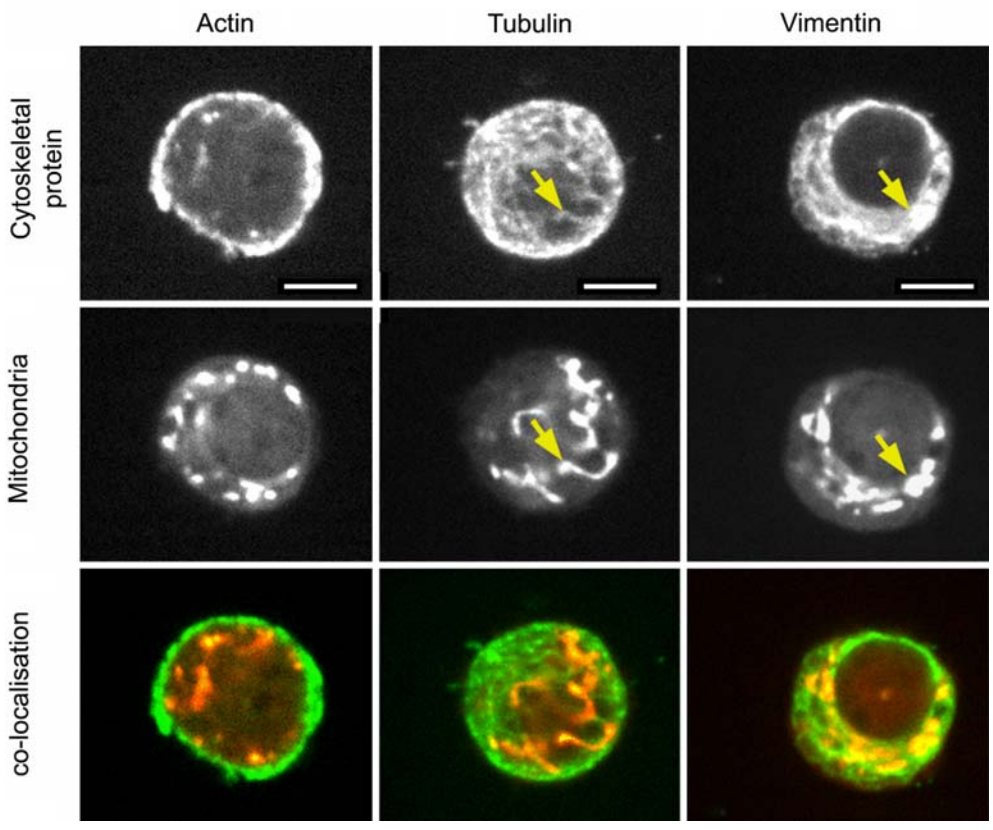

Fig. 3 Co-localisation of mitochondria with three different cytoskeletal proteins in isolated chondrocytes cultured in agarose constructs. Cells were dual labelled for mitochondria and either actin, vimentin or tubulin and visualised using confocal microscopy. *Arrows* indicate examples of co-localisation between the mitochondria and cytoskeleton. *Scale bars* represents 5 μm

cernable fluctuations in cell shape over an 8-min period in the uncompressed agarose constructs (Fig. 4). Gross compression resulted in uniform cell deformation to an elliptical cross section (Fig. 4). Figure 4 shows the confocal images of fluorescently labelled mitochondria and corresponding bright-field images for a single representative cell visualised in the uncompressed state and at incremental levels of gross compression. Digital image correlation was used to calculate the localised intracellular displacements and strains as shown in Fig. 5. DIC revealed a small amount of movement and reorganisation of the mitochondria in uncompressed cells over an 8-minute period. However, cell deformation appeared to produce a greater degree of movement and distortion over the same time period (Figs. 4 and 5). This was confirmed by plotting against time, the median intracellular displacement and strain values calculated for all regions of interest within a cell. The data for a single representative cell is shown in Fig. 6. This figure indicates that incremental levels of compression induced greater intracellular displacements (Fig. 6a) and strains parallel to the axis of compression (Fig. 6b), compared to those values measured in the uncompressed state at the same time point. The differences were statistically significant at 5, 10 and 15% gross compressive strain based on a non parametric Mann–Whitney U-test ($p < 0.05$). By contrast, incremental compression induced no statistically significant difference in the strains measured perpendicular to the axis of compression (Fig. 6c). When considering a population of cells ($n = 8$–10), similar trends were observed (Fig. 7) although there was considerable intercellular heterogeneity in the magnitudes and spatial distributions. Again, statistically significant differences between uncompressed and compressed cells were obtained at gross compressive strains of 5, 10 and 15% for displacements and strains parallel to the axis of compression.

The DIC images of intracellular displacements and strains showed considerable intracellular heterogeneity (Fig. 5). The variability of intracellular displacement or strain magnitude values within a single cell was represented by the interquartile range. The interquartile range values for the displacement and strain were calculated for a sample of cells and the mean interquartile range calculated at each level of applied compression. These mean interquartile ranges were normalised to the corresponding values in the uncompressed state, by subtracting the unstrained value from the strained value. The resulting differences in the interquartile range values were plotted against the level of gross compression (Fig. 8). Statistical analysis indicated that in the compressed state there was significantly greater heterogeneity of displacement at all levels of applied strain ($p < 0.05$) compared to that in the uncompressed cells over the same time period (Fig. 8a).

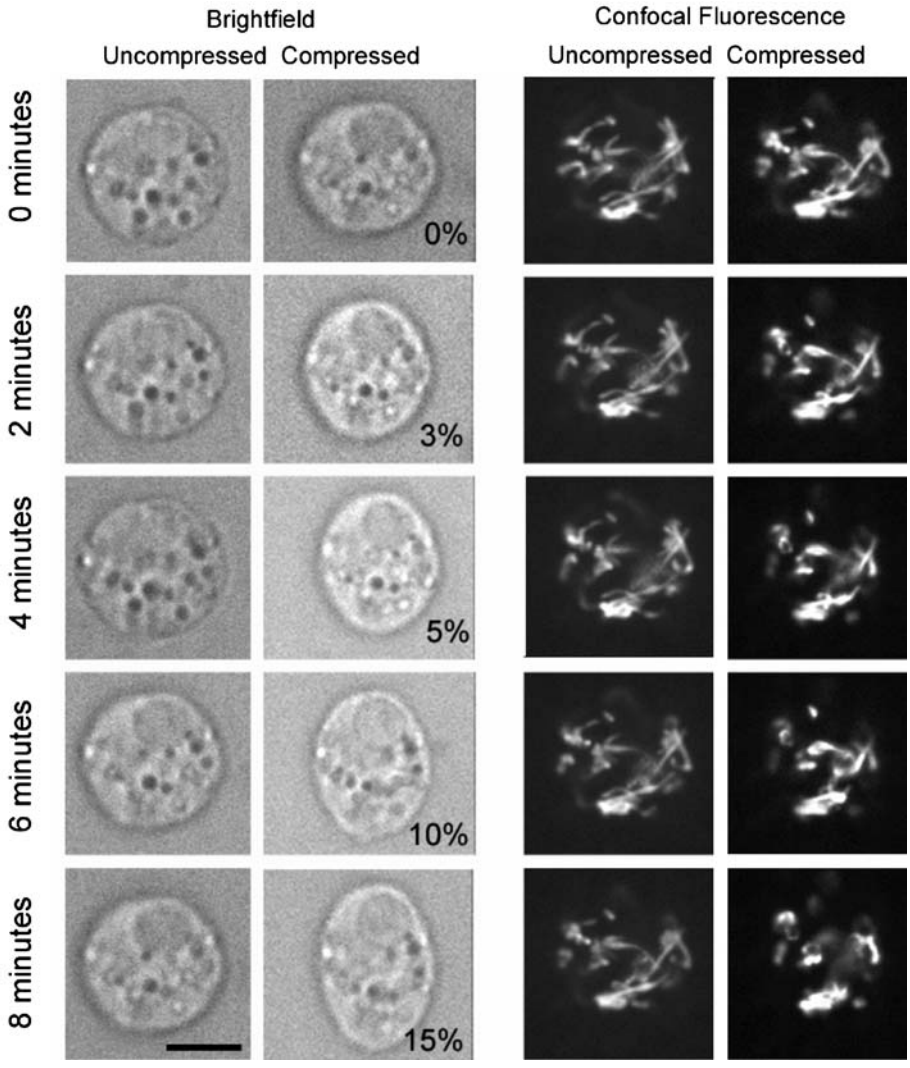

Fig. 4 Brightfield and confocal images bisecting the centre of an individual chondrocyte with fluorescently labelled mitochondria, in an agarose construct. The cell was first visualised in an uncompressed state, with pairs of brightfield and confocal images made at 2-min intervals over an 8-min period. The construct was then subjected to increments of gross compressive strain, applied every 2-min, up to 15% strain. Further pairs of brightfield and confocal images were recorded at each strain increment. The pair of images shown at the end of the uncompressed period (t=8 min) are the same as those shown at the start of the compressed period (t=0 min). *Scale bar* represents 5 μm

Similarly, for intracellular strains measured parallel to the axis of compression, there was a significant trend towards greater heterogeneity in the compressed cells with increasing applied compression (Fig. 8b). The difference from the unstrained state was statistically significant at 15% gross compression. By contrast there was no statistically significant relationship between cell deformation and heterogeneity of strain measurements perpendicular to the axis of compression (Fig. 8c).

3.3 Mitochondrial dynamics in uncompressed and compressed cells

Fast time lapse imaging revealed continuous small scale displacement or movement of the mitochondria within both uncompressed and compressed chondrocytes, although the organisation of the mitochondrial features remained broadly similar over the 10-min period. The movement could be categorised into three modes, namely;

1. Occasional, directional movement of individual mitochondrial segments at speeds of approximately 2 μm/min over distances of up to 4 μm within the confocal plane.
2. 'Wavy movement' within sections of the mitochondrial network.
3. Slow reorganisation of the entire mitochondrial network.

The present study focused on the latter mode of displacement, using the DIC based analysis technique to quantify the magnitude and spatial variability of this movement over a 10-min period. Figure 9 shows the intracellular displacement fields for five representative cells in uncompressed agarose constructs and a separate five cells in statically compressed con-

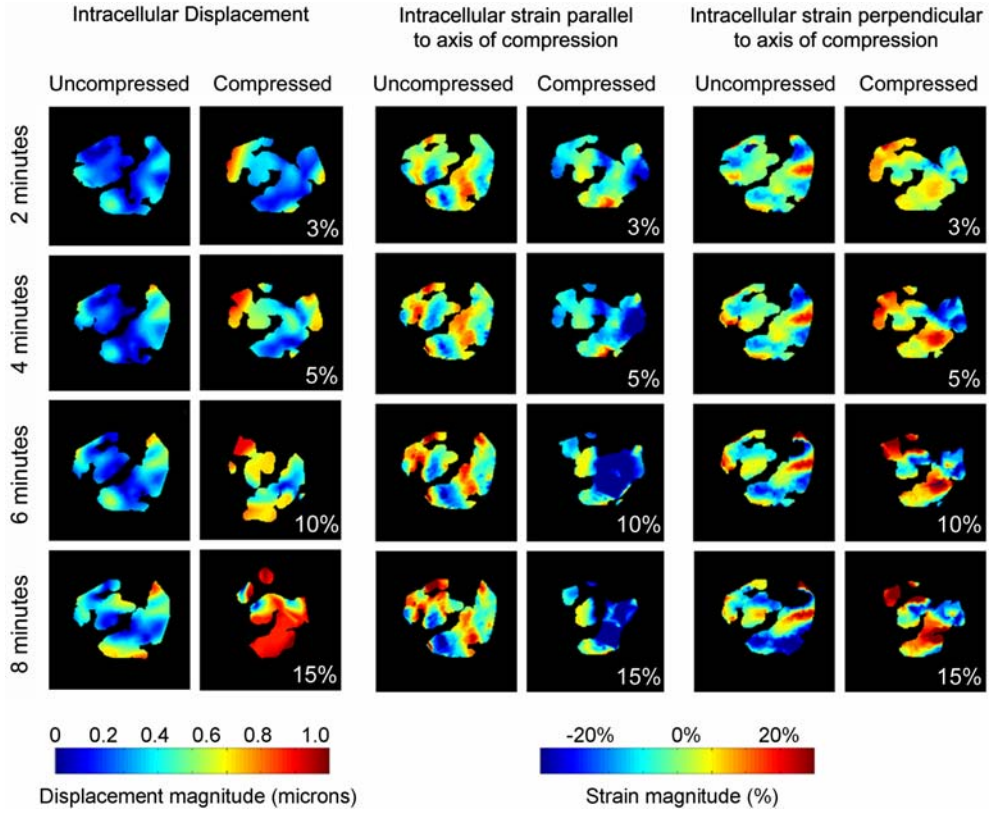

Fig. 5 Psuedocolour images showing the magnitude of intracellular displacements and strains calculated for the representative cell shown in Fig. 4 using digital image correlation as described in the text. Strains have been calculated parallel and perpendicular to the axis of the applied compressive strain. All displacements and strains are calculated relative to the corresponding uncompressed images at t=0 min

structs. The associated displacement measurements suggest considerable intracellular and intercellular heterogeneity.

For each cell, the overall intracellular displacement was estimated as the median value measured for all ROIs. This parameter was used as an estimate of the degree of movement or reorganisation of the mitochondrial reticulum within the individual cell. Based on this approach, there were no statistically significant differences between the degree of overall movement in samples of uncompressed and compressed cells over the 10-min period (ANOVA $p > 0.05$).

4 Discussion

Isolated articular chondrocytes were compressed in agarose constructs using a well characterised experimental system (Sawae et al. 2004; Roberts et al. 2001). All experiments were conducted at day 1 of culture, at which time gross compression has been shown to induce cell deformation from a spherical to an oblate ellipsoid morphology (Lee et al. 2000). Previous studies by the authors used confocal microscopy to accurately measure the level of cell deformation in viable chondrocytes compressed in agarose constructs on the stage of an inverted microscope (Knight et al. 2002). These studies reported that cell strain, in the axis of compression, is equal to the applied strain, indicating that the cell modulus is less than or equal to that of the agarose, given the cell volume fraction of 0.2% (Bader et al. 2002; Knight et al. 2002). Prior to the synthesis of pericellular matrix, gross compression generates identical deformation for all cells due to the heterogeneous properties of the agarose construct (Knight et al. 1998). Despite the uniform mechanical stimuli in compressed agarose constructs, the cellular mechanotransduction response appears to be highly cell-dependent. For example, mechanical compression activates intracellular calcium signalling only in a sub-population of chondrocytes (Roberts et al. 2001). The present study investigated the intercellular variability in the displacements and strains within individual cells, which may contribute to the observed heterogeneity in mechanotransduction. The agarose model is well-suited for these studies due to the homogenous nature of the cell strain produced by gross compression in the absence of significant extracellular matrix. This is in marked contrast to the behaviour in the native cartilage tissue, where gross compression generates heterogeneous levels of cell deformation due to variations in the moduli of the extracellular and pericellular matrix (Guilak et al. 1995).

The mitochondria within viable chondrocytes were fluorescently labelled and visualised using confocal microscopy revealing a dynamic fibrous network or reticulum (Fig. 2), as reported in other cell types (Ball and Singer 1982; Collins et al. 2002; Cambray-Deakin et al. 1988). Co-localisation

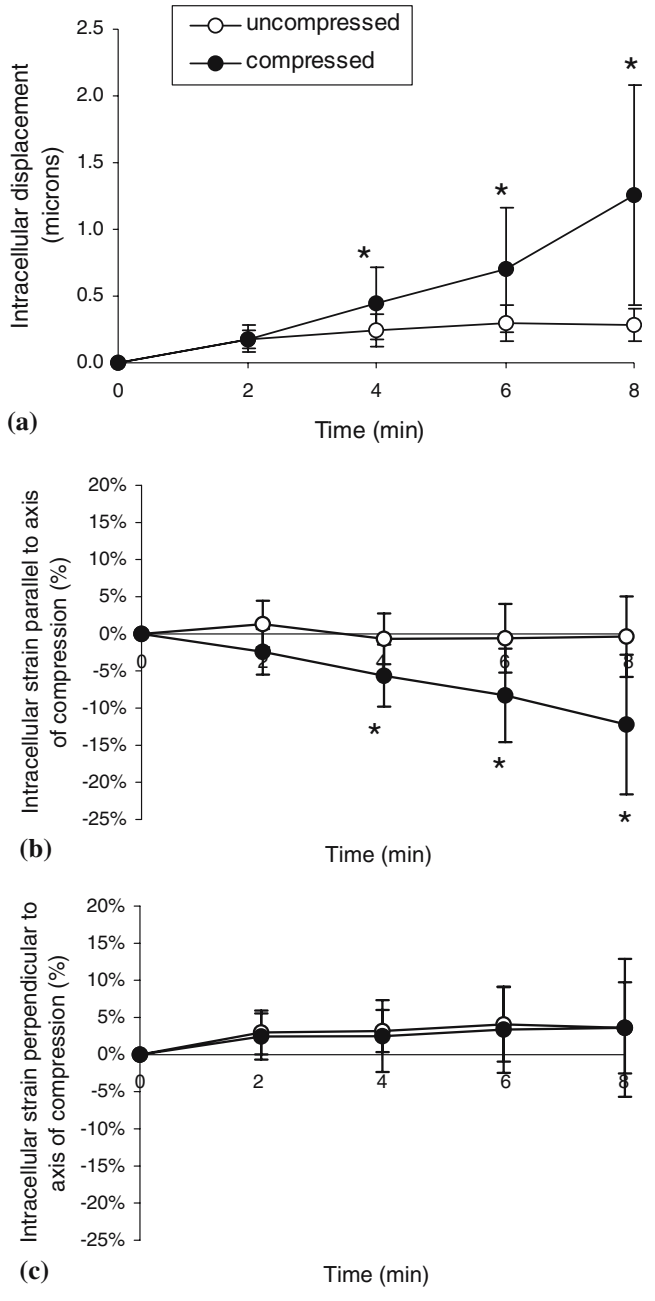

Fig. 6 Intracellular displacement (**a**) and strains parallel (**b**) and perpendicular (**c**) to the axis of gross compression, plotted against time for the individual cell shown in Figs. 4 and 5. Values represent the median intracellular displacement and strain magnitudes with *error bars* indicating interquartile ranges for all convergent regions of interest ($n \approx 400$) within each image. Statistically significant differences from the unstrained state have been indicated ($^*p < 0.05$)

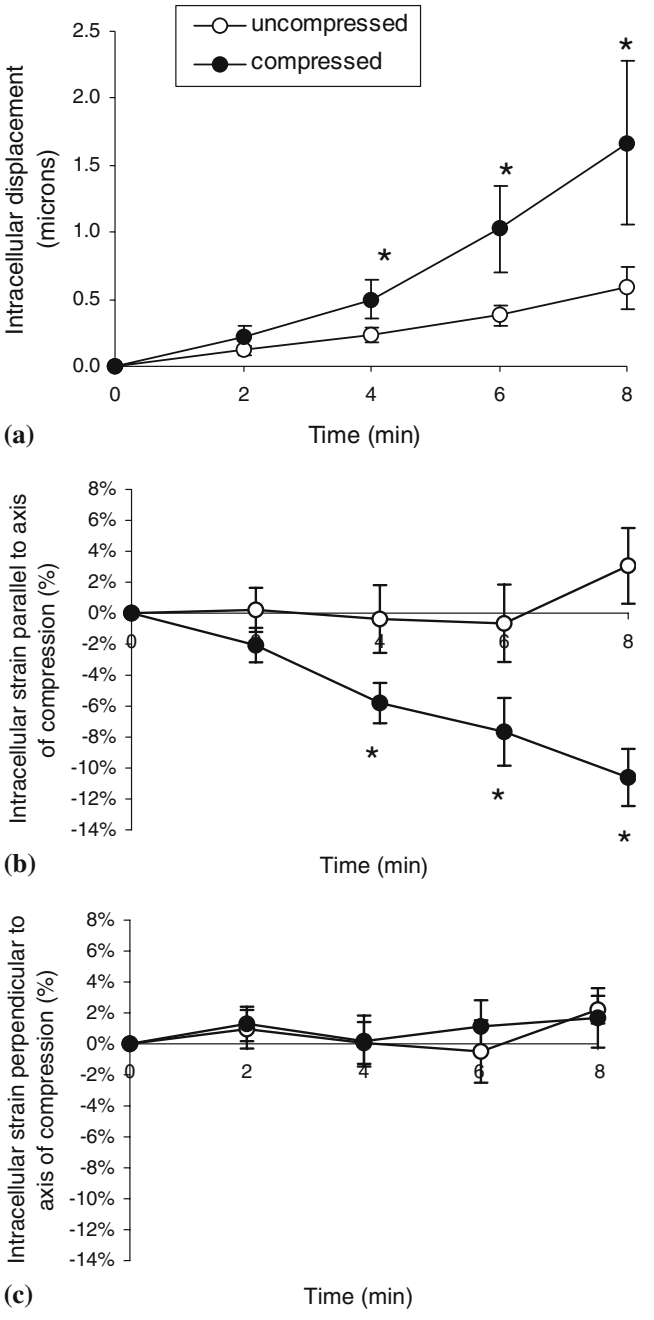

Fig. 7 Average intracellular displacement (**a**) and strain parallel (**b**) and perpendicular (**c**) to the axis of gross compression, plotted against time for the sample of cells. Values represent the sample mean values with error bars indicating SEM ($\boldsymbol{n} = 6-10$). Statistically significant differences from the unstrained state have been indicated ($^*p < 0.05$)

studies indicated that the fibrous mitochondrial structures were partly co-localised with microtubules (Fig. 3), particularly for chondrocytes cultured in monolayer (data not shown). This suggests some degree of association between the two networks as previously reported for other cell types cultured in monolayer (Ball and Singer 1982; Cambray-Deakin et al. 1988). Thus the measurement of mitochondrial network distortion, movement and reorganisation may also provide indirect information on the mechanics of the underlying microtubule and intermediate filament cytoskeleton. The mitochondrial features showed rapid directional movement, as well as a slower 'wavy' movement and more co-ordinated reorganisation. The former is most likely associated with actin–myosin driven movement along microtubules (Krendel et al. 1998), whilst the wavy motion may reflect similar movement previously reported in the underlying cytoskeleton (Ho et al. 1998; Delhaas et al. 2002). The

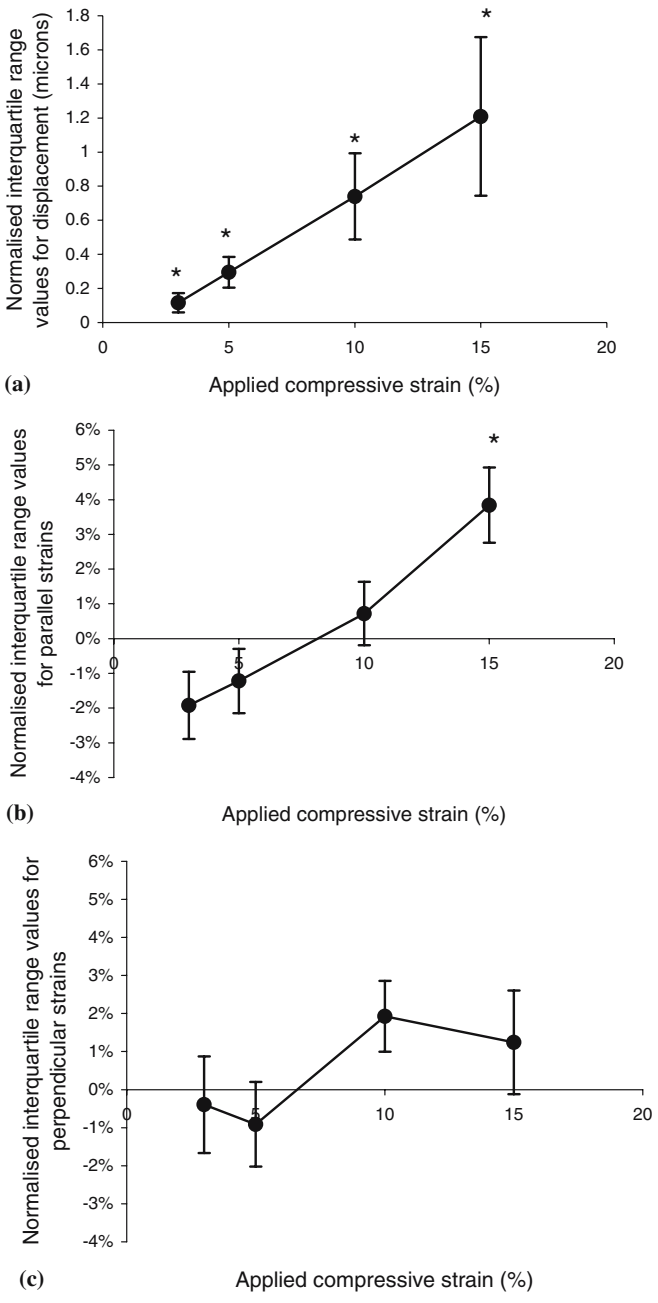

Fig. 8 Intracellular heterogeneity in displacement (**a**) and strain parallel (**b**) and perpendicular (**c**) to the axis of gross compression, for a sample of cells. In each cell, the interquartile range values based on all convergent regions of interest at each level of applied compression have been normalised to the values calculated in the uncompressed state at the equivalent time point (compressed value – uncompressed value). The resulting mean differences in interquartile ranges have been plotted against the level of applied gross compression for the sample of cells. *Error bars* indicate SEM. Statistically significant differences from the unstrained state have been indicated ($*p < 0.05$)

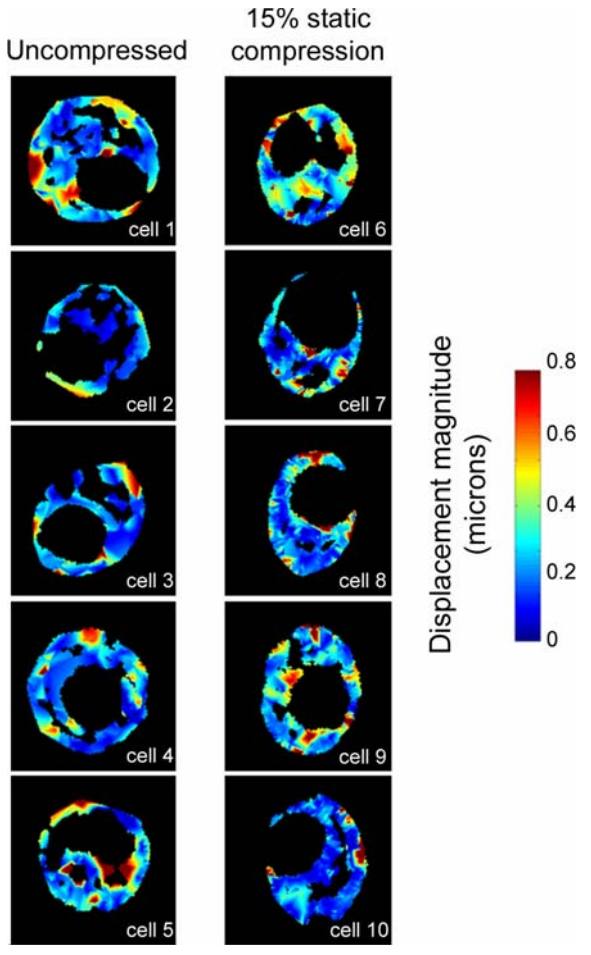

Fig. 9 Psuedocolour images showing the magnitude of intracellular displacements for 10 separate cells visualized over a 10-min period in the uncompressed state or at 15% gross static compression

coordinated reorganisation of the reticulum probably involves a combination of mechanisms.

The distortion of the mitochondria associated with chondrocyte deformation was quantified using DIC, a computational technique for analysing movement and distortion within pairs of images. DIC has previously been used for measuring deformation in a wide range of structures including polymeric foams (Wang and Cuitino 2002), articular cartilage (Wang et al. 2003; Chahine et al. 2004) and trabecular bone (McKinley and Bay 2003). In the present study the technique was optimised for use with confocal images of fluorescently labelled mitochondria within isolated chondrocytes seeded in agarose constructs. Fluorescently labelled mitochondria have previously been used in this manner to calculate the intracellular strain fields in smooth muscle cells (Hu et al. 2003). Alternatively, GFP tagged vimentin intermediate filaments have been used with similar computational techniques to quantify intracellular displacement and strain fields within different cell types cultured in monolayer (Helmke et al. 2000, 2001, 2003; Delhaas et al. 2002). However, to our knowledge, this is the first experimental study to examine the intracellular strain fields associated with physiological mechanical deformation of articular chondrocytes.

Digitial images correlation enabled the calculation of intracellular displacements and strains with sub-pixel resolution. Intracellular displacements and strains parallel and perpendicular to the applied compression were automatically

calculated and graphically displayed in the form of pseudo-colour maps (Fig. 5). The technique was also able to determine the shear strains, area strains, von-Mises strains and the magnitude and direction of the principle strains (data not shown). It should be noted that the term, strain, has been used to indicate a percentage change in dimensions of the mitochondrial network, which may be the result of either mechanical deformation or inherent temporal movement of the mitochondrial features. Validation studies using artificially distorted confocal images showed that the DIC technique was able to produce accurate measurements of intracellular strain.

The present study used a 2D confocal approach for investigating the strain distribution within a cell. However, it is recognised that DIC and other textural correlation methods may detect apparent erroneous 'strains' caused by small changes in the position of the 2D confocal section. To compensate for this potential source of error, results from images captured at increasing levels of applied strain were compared with those obtained for the same cell imaged in the unstrained state. For both unstrained and strained cells, images were refocused at each time increment. Thus the increased strain magnitude and heterogeneity associated with cell deformation are unlikely to be caused by any small variations in confocal plane. Nonetheless, some error may be attributed to compression induced vertical movement of features out of the confocal plane. Future studies might employ a more comprehensive 3D confocal approach, although the associated problems of complexity and poor lateral image resolution would need to be addressed.

The present study employed gross compressive strains up to 15%, which is within the physiological range of strains associated with static compression of cartilage explants (Guilak 1995). Confocal imaging suggested that chondrocyte deformation was associated with movement and distortion of the mitochondrial reticulum, which appeared to collapse in the axis of compression (Figs. 4, 5). This was confirmed by DIC analysis, such that each cell showed greater intracellular displacement and strain parallel to the axis of compression compared to that measured in the uncompressed state over the same time interval (Figs. 6, 7). The differences were statistically significant at applied strains of 5, 10 and 15% ($p < 0.05$). However, there were no statistically significant differences between compressed and uncompressed cells in terms of the strains perpendicular to the axis of compression. This indicates that the mitochondrial reticulum deforms with minimal lateral expansion, suggesting a loss of volume. This finding is in contrast to the deformation of isolated chondrocytes in agarose, which deform with significant lateral expansion and hence maintain their cell volume, based on the validated assumption that the cell deforms to an oblate ellipse (Lee et al. 2000). This agrees with a previous electron microscopy study of chondrocyte deformation in cartilage explants, which suggests that cell deformation is associated with a loss of mitochondrial volume (Szafranski et al. 2004). This previous study hypothesises that the loss of mitochondrial volume is associated with the osmotic reduction in cell and nucleus volume in compressed cartilage (Guilak 1995). However, the data from the present study suggest that the loss of mitochondrial volume is a direct mechanical effect, which occurs independent of the changes in cell volume.

The present study demonstrates that chondrocyte deformation induces mitochondrial distortion indicating a potential role in mechanotransduction. This may occur through strain-mediated release of either nucleotides such as ATP (Graff et al. 2000) or reactive oxygen species (ROS) (Ali et al. 2004; Szafranski et al. 2004). Indeed, articular chondrocytes have been shown to activate intracellular calcium signalling in response to both extracellular ATP (Elfervig et al. 2001) and ROS (Knight et al. 2003). Similar increased calcium signalling has also been reported for isolated chondrocytes compressed in agarose constructs, although the precise mechanisms are as yet unclear (Roberts et al. 2001).

The DIC analysis revealed considerable spatial heterogeneity in intracellular displacement and strain fields within compressed cells (Fig. 5). Thus some areas of the cell experienced local strains several times greater than the applied strain, while other areas experienced minimal strain. The study examined whether this intracellular heterogeneity was due to heterogeneity in intracellular mechanical environment or the inherent heterogeneity caused by mitochondrial motion and remodelling. The variability in displacements and strains in an image was represented by the interquartile range values calculated for all the convergent regions of interest. The interquartile range provides an indication of heterogeneity although it does not directly describe the spatial distribution. Nevertheless, using this parameter, statistical analysis indicated that in compressed cells the variability or heterogeneity was greater than in uncompressed cells for both intracellular displacements and strains measured parallel, but not perpendicular, to the axis of compression (Fig. 8). Consequently, these findings suggest a degree of heterogeneity within the mechanical environment of the cytoplasm, which is frequently overlooked in studies of cell mechanics. The spatial variability is partly associated with the location of the nucleus, which is reported to have a modulus approximately ten times greater than that of the cytoplasm (Guilak et al. 2000). In addition, the local organisation and density of the mitochondrial network and hence the associated microtubule cytoskeleton also appears to influence the intracellular mechanical environment (Figs. 4, 5). Thus, it may be hypothesised that different cells with inherently different intracellular structure and organisation will exhibit heterogeneous intracellular displacement and strain fields. Hence there may be a diversity of response to mechanical stimuli in a cell population despite a uniform level of cell deformation. It is also interesting to note that these intracellular displacements and strains associated with cell deformation occur at day 1 of culture when the cells are surrounded by very little extracellular matrix (Lee et al. 2000). Thus, the presence of matrix is not essential for intracellular strain transfer. However pericellular matrix may modify the intracellular displacement and strain distributions and, hence, small differences in the quantity or

type of pericellular matrix may contribute to the observed intercellular heterogeneity. Although there are clearly other potential causes of chondrocyte heterogeneity, this study describes several possible mechanisms which may contribute to the widely reported intercellular heterogeneity of mechanotransduction behaviour.

It is unclear whether the mitochondrial network distortion associated with cell deformation is reversible, such that repeated cycles of compression produce similar intracellular strain fields. This may trigger coordinated remodelling of the intracellular architecture in response to a repetitive strain field, in a similar manner to the well established Wolff's law observed in bone and other tissues (Hayashi 1996).

The present study examined the influence of cell deformation on mitochondrial dynamics over a 10-min period. Although it is recognised that mitochondrial remodelling may occur over several hours, the short term response to compression provides some indication of the viscoelastic mechanical behaviour. Results indicated no statistically significant difference in the displacement present within uncompressed cells and those held at 15% static compression (Fig. 9), suggesting that static deformation did not trigger significant remodelling or viscoelastic relaxation of the mitochondrial reticulum over the 10-min period. This is in contrast to the compression induced remodelling observed for actin microfilaments (Knight et al., 2002a) and vimentin intermediate filaments (Durrant et al. 1999). However, the mechanical interactions between mitochondria and the cytoskeleton remain unclear, as are the timescales over which any mitochondrial or cytoskeletal remodelling may occur.

In conclusion, the present study describes a series of experimental and computation techniques which have been used to quantify mitochondrial distortion and associated intracellular displacement and strain fields within compressed chondrocytes. In so doing, the study provides important information regarding cell mechanics and the potential role of mitochondrial deformation in chondrocyte mechanotransduction. This analysis demonstrates that cell deformation generates heterogeneous intracellular strain fields which appear to be influenced by cellular structural organisation. This is likely to generate further intercellular heterogeneity in chondrocyte mechanotransduction behaviour.

Acknowledgements Dr. Knight is funded on an EPSRC Advanced Research Fellowship. Dr. Sharma is funded on a BBSRC research grant. The authors would like to thank the meat inspectors at Dawn Cardington for the supply of bovine metacarpal–phalangeal joints.

References

Ali MH, Pearlstein DP, Mathieu CE, Schumacker PT (2004) Mitochondrial requirement for endothelial responses to cyclic strain: implications for mechanotransduction. Am J Physiol Lung Cell Mol Physiol 287:L486–L496

Bader DL, Ohashi T, Knight MM, Lee DA, Sato M (2002) Deformation properties of articular chondrocytes: a critique of three separate techniques. Biorheology 39:69–78

Ball EH, Singer SJ (1982) Mitochondria are associated with microtubules and not with intermediate filaments in cultured fibroblasts. Proc Natl Acad Sci USA 79:123–126

Cambray-Deakin MA, Robson SJ, Burgoyne RD (1988) Colocalisation of acetylated microtubules, glial filaments, and mitochondria in astrocytes in vitro. Cell Motil Cytoskeleton 10:438–449

Chahine NO, Wang CC, Hung CT, Ateshian GA (2004) Anisotropic strain-dependent material properties of bovine articular cartilage in the transitional range from tension to compression. J Biomech 37:1251–1261

Collins TJ, Berridge MJ, Lipp P, Bootman MD (2002) Mitochondria are morphologically and functionally heterogeneous within cells. EMBO J 21:1616–1627

D'Andrea P, Calabrese A, Capozzi I, Grandolfo M, Tonon R, Vittur F (2000) Intercellular Ca2+ waves in mechanically stimulated articular chondrocytes. Biorheology 37:75–83

Delhaas T, Van Engeland S, Broers J, Bouten C, Kuijpers N, Ramaekers F, Snoeckx LH (2002) Quantification of cytoskeletal deformation in living cells based on hierarchical feature vector matching. Am J Physiol Cell Physiol 283:C639–C645

Durrant LA, Archer CW, Benjamin M, Ralphs JR (1999) Organisation of the chondrocyte cytoskeleton and its response to changing mechanical conditions in organ culture. J Anat 194:343–353

Elfervig MK, Graff RD, Lee GM, Kelley SS, Sood A, Banes AJ (2001) ATP induces Ca(2+) signaling in human chondrons cultured in three-dimensional agarose films. Osteoarthr Cartil 9:518–526

Graff RD, Lazarowski ER, Banes AJ, Lee GM (2000) ATP release by mechanically loaded porcine chondrons in pellet culture. Arthritis Rheum 43:1571–1579

Guilak F (1995) Compression-induced changes in the shape and volume of the chondrocyte nucleus. J Biomech 28:1529–1541

Guilak F, Ratcliffe A, Mow VC (1995) Chondrocyte deformation and local tissue strain in articular cartilage: A confocal microscopy study. J Orthop Res 13:410–421

Guilak F, Zell RA, Erickson GR, Grande DA, Rubin CT, McLeod KJ, Donahue HJ (1999) Mechanically induced calcium waves in articular chondrocytes are inhibited by gadolinium and amiloride. J Orthop Res 17:421–429

Guilak F, Tedrow JR, Burgkart R (2000) Viscoelastic properties of the cell nucleus. Biochem Biophys Res Commun 269:781–786

Hayashi K (1996) Biomechanical studies of the remodeling of knee joint tendons and ligaments. J Biomech 29:707–716

Helmke BP, Goldman RD, Davies PF (2000) Rapid displacement of vimentin intermediate filaments in living endothelial cells exposed to flow. Circ Res 86:745–752

Helmke BP, Rosen AB, Davies PF (2003) Mapping mechanical strain of an endogenous cytoskeletal network in living endothelial cells. Biophys J 84:2691–2699

Helmke BP, Thakker DB, Goldman RD, Davies PF (2001) Spatiotemporal analysis of flow-induced intermediate filament displacement in living endothelial cells. Biophys J 80:184–194

Ho CL, Martys JL, Mikhailov A, Gundersen GG, Liem RK (1998) Novel features of intermediate filament dynamics revealed by green fluorescent protein chimeras. J Cell Sci 111:1767–1778

Hu S, Chen J, Fabry B, Numaguchi Y, Gouldstone A, Ingber DE, Fredberg JJ, Butler JP, Wang N (2003) Intracellular stress tomography reveals stress focusing and structural anisotropy in cytoskeleton of living cells. Am J Physiol Cell Physiol 285:C1082–C1090

Idowu BD, Knight MM, Bader DL, Lee DA (2000) Confocal analysis of cytoskeletal organisation within isolated chondrocyte sub-populations cultured in agarose. Histochem J 32:165–174

Knight MM, Lee DA, Bader DL (1998) The influence of elaborated pericellular matrix on the deformation of isolated articular chondrocytes cultured in agarose. Biochim Biophys Acta 1405:67–77

Knight MM, van de Breevaart BJ, Lee DA, van Osch GJ, Weinans H, Bader DL (2002) Cell and nucleus deformation in compressed chondrocyte-alginate constructs: temporal changes and calculation of cell modulus. Biochim Biophys Acta 1570:1–8

Knight MM, Roberts SR, Lee DA, Bader DL (2003) Live cell imaging using confocal microscopy induces intracellular calcium transients and cell death. Am J Physiol Cell Physiol 284:C1083–C1089

Knight MM, Toyoda T, Lee DA, Bader DL (2006) Mechanical strain and hydrostatic pressure induce reversible changes in actin cytoskeletal organisation in chondrocytes in agarose. J Biomech (in Press)

Krendel M, Sgourdas G, Bonder EM (1998) Disassembly of actin filaments leads to increased rate and frequency of mitochondrial movement along microtubules. Cell Motil Cytoskeleton 40:368–378

Lee DA, Bader DL (1997) Compressive strains at physiological frequencies influence the metabolism of chondrocytes seeded in agarose. J Orthop Res 15:181–188

Lee DA, Knight MM, Bolton JF, Idowu BD, Kayser MV, Bader DL (2000) Chondrocyte deformation within compressed agarose constructs at the cellular and sub-cellular levels. J Biomech 33:81–95

McKinley TO, Bay BK (2003) Trabecular bone strain changes associated with subchondral stiffening of the proximal tibia. J Biomech 36:155–163

Millward-Sadler SJ, Salter DM (2004) Integrin-dependent signal cascades in chondrocyte mechanotransduction. Ann Biomed Eng 32:435–446

Mobasheri A, Carter SD, Martin-Vasallo P, Shakibaei M (2002) Integrins and stretch activated ion channels; putative components of functional cell surface mechanoreceptors in articular chondrocytes. Cell Biol Int 26:1–18

Roberts SR, Knight MM, Lee DA, Bader DL (2001) Mechanical compression influences intracellular Ca^{2+} signaling in chondrocytes seeded in agarose constructs. J Appl Physiol 90:1385–1391

Sawae Y, Shelton JC, Bader DL, Knight MM (2004) Confocal analysis of local and cellular strains in chondrocyte-agarose constructs subjected to mechanical shear. Ann Biomed Eng 32:860–870

Szafranski JD, Grodzinsky AJ, Burger E, Gaschen V, Hung HH, Hunziker EB (2004) Chondrocyte mechanotransduction: effects of compression on deformation of intracellular organelles and relevance to cellular biosynthesis. Osteoarthr Cartil 12:937–946

Urban JPG (1994) The chondrocyte: A cell under pressure. Br J Rheumatol 33:901–908

Wang CC, Chahine NO, Hung CT, Ateshian GA (2003) Optical determination of anisotropic material properties of bovine articular cartilage in compression. J Biomech 36:339–353

Wang Y, Cuitino AM (2002) Full-field measurements of heterogeneous deformation patterns on polymeric foams using digital image correlation. Int J Sol Struct 39:3777–3796